学位論文

Digital PCR-based plasma cell-free DNA mutation analysis for early-stage pancreatic tumor diagnosis and surveillance

(デジタルPCRを用いた遺伝子変異解析による膵腫瘍の早期診断とサーベイランス)

旭川医科大学医学部
旭川医科大学大学院医学系研究科博士課程
臨床腫瘍・血液学（地域臨床腫瘍医養成PG）専攻

岡田　哲弘

(Yusuke Mizukami, Yusuke Ono, Hiroki Sato, Akihiro Hayashi, Hidemasa Kawabata, Kazuya Koizumi, Sakue Masuda, Shinichi Teshima, Kuniyuki Takahashi, Akio Katanuma, Yuko Omori, Hirotoshi Iwano, Masataka Yamada, Tomoki Yokochi, Shingo Asahara, Kazumichi Kawakubo,Masaki Kuwatani, Naoya Sakamoto, Katsuro Enomoto, Takuma Goto,Junpei Sasajima, Mikihiro Fujiya, Jun Ueda, Seiji Matsumoto, Kenzui Taniue, Ayumu Sugitani, Hidenori Karasaki & Toshikatsu Okumura)

J Gastroenterol
https://doi.org/10.1007/s00535-020-01724-5

The Japanese Society of Gastroenterology

ORIGINAL ARTICLE—LIVER, PANCREAS, AND BILIARY TRACT

Digital PCR-based plasma cell-free DNA mutation analysis for early-stage pancreatic tumor diagnosis and surveillance

Tetsuhiro Okada[1,2] · Yusuke Mizukami[1,2] · Yusuke Ono[1,2] · Hiroki Sato[2] · Akihiro Hayashi[2] · Hidemasa Kawabata[2] · Kazuya Koizumi[3] · Sakue Masuda[3] · Shinichi Teshima[4] · Kuniyuki Takahashi[5] · Akio Katanuma[5] · Yuko Omori[6] · Hirotoshi Iwano[7] · Masataka Yamada[7] · Tomoki Yokochi[8] · Shingo Asahara[8] · Kazumichi Kawakubo[9] · Masaki Kuwatani[9] · Naoya Sakamoto[9] · Katsuro Enomoto[2] · Takuma Goto[2] · Junpei Sasajima[1,2] · Mikihiro Fujiya[2] · Jun Ueda[10] · Seiji Matsumoto[10] · Kenzui Taniue[1] · Ayumu Sugitani[1] · Hidenori Karasaki[1] · Toshikatsu Okumura[2]

Received: 20 April 2020 / Accepted: 17 August 2020

Abstract

Background Cell-free DNA (cfDNA) shed from tumors into the circulation offers a tool for cancer detection. Here, we evaluated the feasibility of cfDNA measurement and utility of digital PCR (dPCR)-based assays, which reduce subsampling error, for diagnosing pancreatic ductal adenocarcinoma (PDA) and surveillance of intraductal papillary mucinous neoplasm (IPMN).

Methods We collected plasma from seven institutions for cfDNA measurements. Hot-spot mutations in *KRAS* and *GNAS* in the cfDNA from patients with PDA (n = 96), undergoing surveillance for IPMN (n = 112), and normal controls (n = 76) were evaluated using pre-amplification dPCR.

Results Upon Qubit measurement and copy number assessment of hemoglobin-subunit (*HBB*) and mitochondrially encoded NADH:ubiquinone oxidoreductase core subunit 1 (*MT-ND1*) in plasma cfDNA, *HBB* offered the best resolution between patients with PDA relative to healthy subjects [area under the curve (AUC) 0.862], whereas *MT-ND1* revealed significant differences between IPMN and controls (AUC 0.851). DPCR utilizing pre-amplification cfDNA afforded accurate tumor-derived mutant *KRAS* detection in plasma in resectable PDA (AUC 0.861–0.876) and improved post-resection recurrence prediction [hazard ratio (HR) 3.179, 95% confidence interval (CI) 1.025–9.859] over that for the marker CA19-9 (HR 1.464; 95% CI 0.674–3.181). Capturing *KRAS* and *GNAS* could also provide genetic evidence in patients with IPMN-associated PDA and undergoing pancreatic surveillance.

Conclusions Plasma cfDNA quantification by distinct measurements is useful to predict tumor burden. Through appropriate methods, dPCR-mediated mutation detection in

Electronic supplementary material The online version of this article (https://doi.org/10.1007/s00535-020-01724-5) contains supplementary material, which is available to authorized users.

✉ Yusuke Mizukami
mizu@asahikawa-med.ac.jp

1 Institute of Biomedical Research, Sapporo Higashi Tokushukai Hospital, Sapporo, Japan

2 Division of Gastroenterology and Hematology/Oncology, Department of Medicine, Asahikawa Medical University, 2-1 Midorigaoka Higashi, Asahikawa, Hokkaido 078-8510, Japan

3 Center for Gastroenterology, Shonan Kamakura General Hospital, Kamakura, Japan

4 Department of Pathology, Shonan Kamakura General Hospital, Kamakura, Japan

5 Center for Gastroenterology, Teine-Keijinkai Hospital, Sapporo, Japan

6 Department of Pathology, Teine-Keijinkai Hospital, Sapporo, Japan

7 Department of Gastroenterology and Endoscopic Unit, Shibetsu City Hospital, Shibetsu, Japan

8 Department of Clinical Research, Chiba Tokushukai Hospital, Funabashi, Japan

9 Department of Gastroenterology and Hepatology, Hokkaido University Graduate School of Medicine, Sapporo, Japan

10 Center for Advanced Research and Education, Asahikawa Medical University, Asahikawa, Japan

Published online: 16 September 2020

patients with localized PDA and IPMN likely to progress to invasive carcinoma is feasible and complements conventional biomarkers.

Keywords Pancreatic cancer · Liquid biopsy · Cell-free DNA · Digital PCR · Risk assessment

Introduction

Pancreatic ductal adenocarcinomas (PDAs) are among the deadliest types of cancers worldwide. To improve the prognosis of PDA, development of new biomarkers that enable early detection represents an urgent issue. In human PDAs, mutations in *KRAS* are found in over 90% of patients [1]. Notably, both of the two morphologically distinct types of precursor lesion, termed pancreatic intraepithelial neoplasia and intraductal papillary mucinous neoplasm (IPMN), harbor mutant *KRAS* at 90–95% and 40–75% frequency, respectively [2]. Considerable efforts have, thus, been made to detect oncogenic *KRAS* for early diagnosis and surveillance in high-risk individuals [3, 4]. Similarly, *GNAS*, another oncogene that is specifically mutated in IPMN [5, 6], may also be useful for screening and early detection of related cancers [7].

Technologies for capturing cancer-associated genetic abnormalities using body fluids have been extensively studied [8]. In particular, measurement of cell-free DNA (cfDNA) in plasma constitutes a promising screening tool; however, the mutation detection rates in patients with PDA are less than those in patients with other major types of cancers [9], even in metastatic PDA [10, 11]. Given the low yield of circulating plasma cfDNA specifically in patients with non-metastatic PDA, early detection of tumor-derived DNA by liquid biopsy remains challenging [12]. Advances in technology may provide a solution to overcome the issue; one such promising approach involves molecular barcodes, which minimize sequence-dependent bias [13], although the associated high cost may preclude its use for routine examination. As an alternative, we developed a sensitive and low-cost assay termed the pre-amplification protocol for digital PCR (dPCR) to resolve subsampling error [14]. In brief, we conduct a low-cycle-number pre-amplification step, analyzing 3–4 mL plasma in duplicate/triplicate to avoid subsampling error, and then stop the reaction and extract DNA from the entire pool of droplets, specifically for the enrichment of reactions with very low abundance targets. This pooling effectively dilutes out PCR errors arising in single droplets. Subsequent mutation detection is performed using very sensitive locked nucleic acid (LNA) probes, which improves mismatch discrimination [15].

In this study, we recruited patients with PDA, primarily at surgically resectable stages, and IPMN of various grades as categorized by imaging modalities [16, 17] to examine whether the dPCR-based assay might be applied to the diagnosis of pancreatic neoplasms at curative stages. Validation of this approach will provide the foundation for the implementation of a low-cost, rapid-turn-around screen for diagnostics of pancreatic tumors with prognostic relevance and patient stratification.

Methods

We examined the utility of plasma cfDNA quantification and testing for mutant *KRAS* and *GNAS* in patients with PDA ($n = 96$) and IPMN of the pancreas ($n = 112$) (Table 1) diagnosed between 2015 and 2018 at seven participating institutions acting as regional referral centers for pancreatic diseases (Supplementary Methods). In this observational study, genetic data were analyzed in a blinded manner, without knowledge of information regarding clinical diagnosis or patient outcome. Cases presenting pancreatic cyst not associated with the pancreatic ductal system were excluded. This study was approved by the Tokushukai Group ethical committee on human research (#TGE00357-012) and Institutional Review Boards of other collaborating hospitals and was conducted in accordance with the Declaration of Helsinki. Written informed consent was obtained from all patients prior to enrollment.

PDA stage was determined histologically for resected cases ($n = 66$) or by imaging modalities for unresectable cases ($n = 30$) by pathologists at each institution according to the eighth edition of the Union for International Cancer Control (UICC) [18]. For assessing IPMN grade, the revised Fukuoka criteria were utilized [16].

We collected blood samples (limited to 16 mL), surgically resected primary tumors, and specimens obtained by endoscopic ultrasound-guided fine needle biopsy for unresected PDAs. Plasma cfDNA and tumor DNA were analyzed as we reported previously [14, 19]. (Supplementary Methods). In brief, we conducted an 8-cycle pre-amplification step, analyzing 3–4 mL plasma in duplicate/triplicate to avoid subsampling error, and then stopped the reaction and extracted DNA from the entire pool of droplets. This pooling effectively diluted out PCR errors arising in single droplets; moreover, subsequent mutation detection was performed using highly sensitive LNA probes, as we previously reported [14]. For mutant *KRAS* detection, we utilized two probe sets: G12D/V/C, G13D for pool#1, and G12R/S/A, G13C for pool#2. *GNAS* mutations R201C and R201H were analyzed using a single probe set.

Association significance was assessed using Fisher's exact test for categorical data; continuous data were compared between groups using the Mann–Whitney *U* test. Cut-off values were calculated using the receiver operating

Table 1 Demographic and clinicopathological features of patients and participants

	Controls (healthy volunteers)	IPMN			PDA	
		Fukuoka negative	Worrisome features	High-risk stigmata	Resectable	Unresectable
Number of cases	76	66	37	9	66	30
Age (years)	42.0 (20–64)	71.0 (60–94)	77.5 (48–96)	68.0 (66–90)	71 (44–87)	68 (46–87)
Gender: male/female	38/38	24/42	20/17	4/5	31/35	11/19
Follow-up time [days (IQR)]	NA	382.0 (97.0–963.0)	374.5 (328.0–531.0)	351.0 (315.0–707.0)	–	–
Emergence of PDA (*N*[a])		1[a]	0	2		
Serum CA 19–9 level [U/mL (IQR)]	NA	12.6 (8.4–23.0)	16.0 (10.1–32.4)	22.0 (11.3–23.3)	52 (18.9–210.2)	397.5 (73.1–1612.6)
Number of cases ≥ 55	NA	3/62 (4.8%)	4/34 (11.8%)	2/6 (33.3%)	32/64 (50.0%)	21/28 (75.0%)

Values indicate median unless otherwise stated

IQR interquartile range, *PDA* pancreatic ductal adenocarcinoma, *NA* data not available

[a]The patient enrolled as IPMN and subsequently diagnosed as PDA was also categorized as resectable PDA

characteristic (ROC) curve by Youden's index. The Cochran–Armitage test or Jonckheere–Terpstra test for trend was used when analyzing categorical (tumor cellularity group) or continuous (mutant allele frequency; MAF) data, respectively. For patients with surgically resected PDA, disease-free survival was defined as the time from surgery to that of recurrence and emergence of new neoplastic lesions requiring intervention or the period of last follow-up. We constructed Kaplan–Meier curves and Cox proportional-hazard regression models. Statistical or bioinformatics analyses were performed using a two-sided, 5% significance level and 95% confidence interval (CI) utilizing R (version 3.3.2; The R Foundation, https://www.r-project.org/about.html) and GraphPad Prism (version 8; GraphPad Software, San Diego, CA).

Results

CfDNA quantification and biology

Although cancer generally exhibits higher plasma cfDNA levels than that in healthy subjects, the yield varies considerably [8]. To evaluate whether plasma cfDNA measurements might be affected by tumor grade and burden, we utilized different quantification methods. To obtain real-world data for practical genetic testing, we collected the plasma of patients with IPMN or resectable and unresectable PDA, and control subjects from seven regional hospitals. cfDNA was purified after shipping and quantified using a Qubit fluorometer along with in-house PCR-based methods.

The cfDNA concentration by Qubit revealed a step-wise increase from IPMN to resectable and unresectable PDA relative to control levels (Fig. 1a). IPMN differed slightly albeit significantly from the healthy control samples. CfDNA measurements or CA19-9 did not differ among IPMN subsets clinically categorized by Fukuoka criteria [16], i.e., high-risk stigmata (HRS), worrisome features (WF), and Fukuoka negative (FN), regardless of clear difference in the neutrophil-to-lymphocyte ratio, which comprise previously described predictive markers for the presence of IPMN-associated invasive carcinoma (Supplementary Fig. 1) [20].

The diagnostic power of cfDNA quantity was tested using ROC analysis. The calculated ROC area under the curve (AUC) between control and PDA samples was 0.767 (95% CI 0.697–0.837). Diagnostic accuracy was highest using a threshold of 14.4 ng/mL plasma, providing high specificity (91.8%). Conversely, diagnostic accuracy between controls and IPMN, or IPMN and PDA was weak (Fig. 1a).

PCR-based assays measuring both nuclear (*HBB*) and mitochondrial (*MT-ND1*) DNA copy number in plasma cfDNA showed a similar trend as observed for Qubit measurement (Fig. 1b, c). *HBB* copy number strongly correlated with Qubit quantification, whereas *MT-ND1* copy number weakly associated with Qubit assay results (Supplementary Fig. 2A). *HBB* copy number, therefore, appeared to afford the best accuracy to distinguish patients with PDA from controls (AUC 0.843), whereas *MT-ND1* better resolved patients with IPMN and controls (AUC 0.877) (Fig. 1b, c). Patients with PDA and IPMN showed a steeper slope of the regression line between *HBB* copy

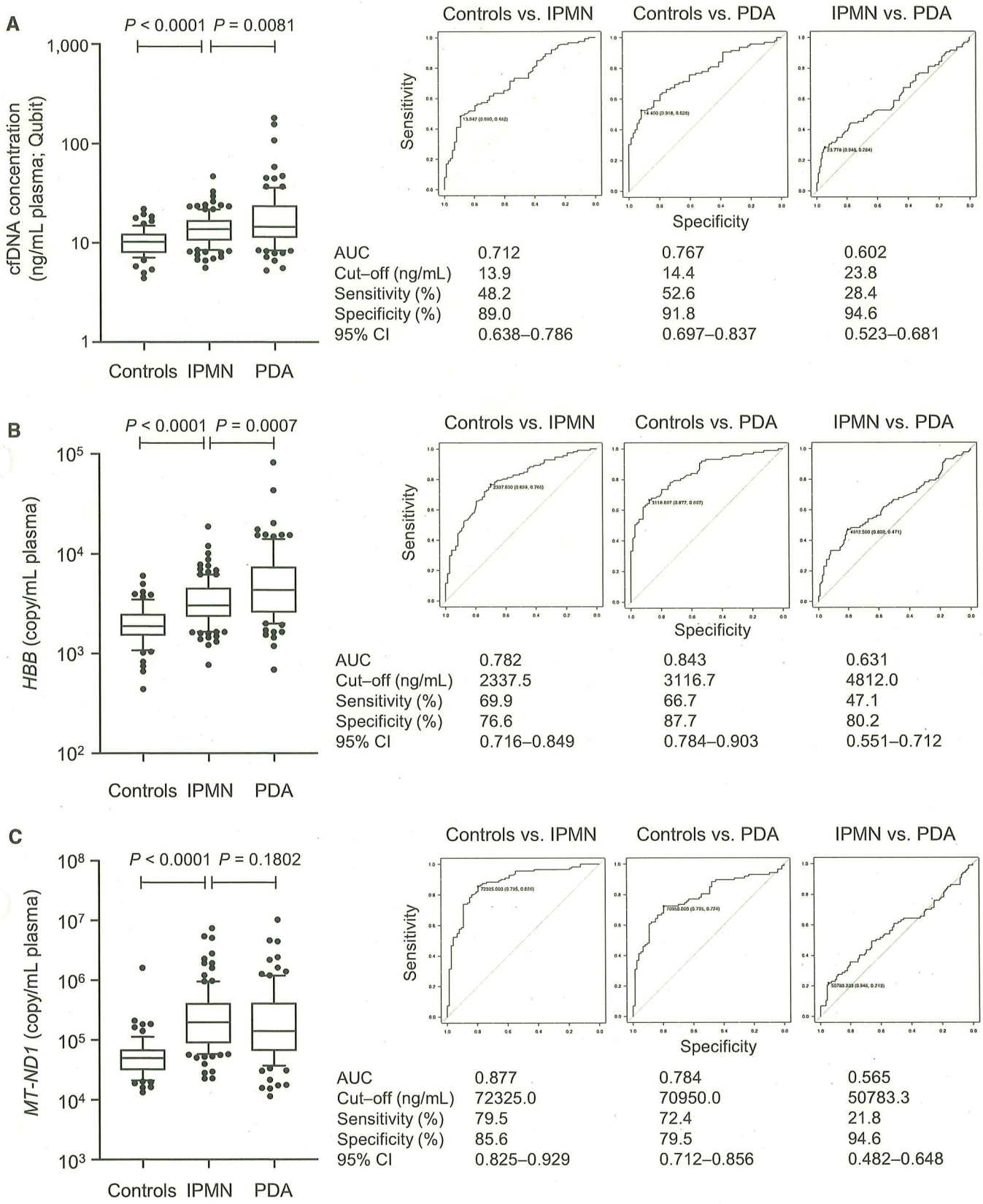

Fig. 1 Results of quantification and ROC curve analysis of plasma cfDNA in controls (n = 76), IPMN (n = 112), and PDA (n = 96). Quantification of cfDNA concentration and ROC curve analysis of the measurements for predicting PDA presence or absence using Qubit (**a**) and dPCR assay targeting *HBB* and *MT-ND1* (**b**, **c**). The box-and-whiskers graphs show median, interquartile, and 10–90% ranges. Data were compared between groups using the Mann–Whitney U test

number and Qubit assay results than that of controls ($P = 0.0139$ and $P = 0.0077$, respectively), whereas those of patients with PDA and IPMN did not significantly differ ($P = 0.2263$) (Supplementary Fig. 2B).

KRAS mutation analysis in PDA tissue and plasma cfDNA

To evaluate whether an improved dPCR protocol that overcomes subsampling errors via a pre-amplification step may affect mutant *KRAS* detection in patients with pancreatic cancer [14], we tested tumor and cfDNA from PDA cases with metastatic disease (i.e., stage IV) (Fig. 2a, Supplementary Tables 1, 2). ROC curve analyses of the mutant *KRAS* allele frequency measured via the pre-amplification assay revealed the AUC for classifying patients with *KRAS* mutant PDA and controls as 90.3% (95% CI 83.4–97.2) and 85.5% (95% CI 69.6–100) for pool#1 and pool#2, respectively, a significant improvement over standard dPCR assay-based scores (Fig. 2b). The optimal cut-off values for pool#1 and pool#2 based on the Youden's index were 0.078% and 0.042%, respectively. The rate of *KRAS* mutation detection in the plasma cfDNA was significantly lower in the PDA cases with locally advanced or peritoneal metastasis than that in patients with metastasis to distant organs (e.g., the liver and lung), whereas measurements obtained using the Qubit assay and *HBB/MT-ND1* copy number quantification revealed no significant differences (Fig. 2c, Supplementary Fig. 3). To afford better specificity in the broader cohort including patients with earlier PDA stages, the cut-off value was determined as 0.1% for subsequent studies for both pool assays (pool#1: sensitivity 69.2% and specificity 97.8%; pool#2: sensitivity 50.0% and specificity 97.8%).

We next tested the pre-amplification protocol in patients with surgically resected PDAs. These patients exhibited lower Qubit measurements of cfDNA levels than those from patients with metastatic disease, whereas *HBB* and *MT-ND1* copy numbers did not significantly differ (Supplementary Fig. 4, Supplementary Table 3). The majority of the resected PDAs comprised Stage II and III disease, with mutant *KRAS* in plasma cfDNA detected in 27 of 38 cases with *KRAS* mutant tumors (71.1%; Fig. 3a). Pre-amplification also captured mutant *KRAS* in PDA with lower tumor burden [2 of 4 (50%) in Stage 0 and 6 of 9 (66.7%) in Stage I] (Fig. 3a, b). Positive detection of mutant *KRAS* in plasma cfDNA was associated with tumor cellularity (Cochran–Armitage trend test; $P = 0.0046$). Cases were identified exhibiting high *KRAS* MAF (> 1%) in later stages (II–III) but not in earlier stages (0–I); however, no significant association was observed between *KRAS* MAF and tumor stage or with pathological T-factor or node presence (Fig. 3b, Supplementary Fig. 5). We also examined whether tumor cellularity might affect the sensitivity for capturing tumor cell-derived cfDNA. Patients with PDA exhibiting > 10% *KRAS* MAF, suggestive of tumor cellularity beyond 20%, exhibited significantly higher frequency of positive mutation calls over 0.1% in plasma cfDNA than that in patients with a lower tumor MAF (Cochran–Armitage trend test; $P = 0.0046$; Fig. 3b). *KRAS* MAF was not associated with CA19-9 levels prior to surgical resection (Fig. 3c). *KRAS* mutations were detected in 16 (64%) of 25 patients with CA19-9-low (below 55 U/mL) [21] resectable PDA, comparable to the sensitivity in CA19-9-high cases (18/27; 66.7%) (Fig. 3c).

We next evaluated whether *KRAS* mutation allele frequency might serve as a prognostic factor for recurrence following surgical resection. Although we found no significant difference between presence (*KRAS* MAF > 0.1%) and absence of mutant *KRAS* calls in plasma cfDNA (Supplementary Fig. 6A), patients with an MAF > 0.45% exhibited significantly shorter disease-free survival than those with lower MAF (HR 3.179, 95% CI 1.025–9.859; $P = 0.0452$) (Fig. 3d). Similar trends were observed in overall survival, albeit at no significance (Supplementary Fig. 6B). Disease-free survival did not significantly differ between patients with high- and low-CA19-9 prior to surgical resection (HR 1.464, 95% CI 0.674–3.181; $P = 0.3362$). Notably, albeit at lower significance, prolonged disease-free survival was observed following surgical resection in patients with *HBB*-low PDA relative to that in the *HBB*-high subset (HR 1.989, 95% CI 0.8553–4.627; $P = 0.0512$), whereas *MT-ND1* levels indicated the opposite trend (HR 0.4034, 95% CI 0.1458–1.116; $P = 0.2010$) (Supplementary Fig. 6B).

KRAS and *GNAS* mutation quantification in IPMN

We then sought to confirm the utility of cfDNA genotyping in the subset of patients with IPMN potentially carrying an enhanced risk to develop cancer. Tumor tissue genotyping using representative invasive compartment specimens among the 21 patients with IPMN-related PDA revealed that 81% (17/21) and 48% (10/21) exhibited *KRAS* and *GNAS* mutation positivity, respectively (Fig. 4a, Supplementary Table 3, Supplementary Fig. 7). Concordance of the genomic findings from the index tumor and plasma cfDNA was 81.3% (over 0.1% in 13 of 16) and 55.5% (over 0.05% in 5 of 9) for the respective genes. In comparison, the modified dPCR assay captured *KRAS* and *GNAS* mutations in 11.1% (2/18) and 41.1% (7/17) of plasma cfDNA from these patients lacking mutations in the primary PDAs. Alternatively, most *KRAS* (5/6) and *GNAS* (2/2) mutations present in the concurrent co-existing tumor (e.g., non-invasive concurrent lesions) but not in the invasive foci (index tumor) were detected in the plasma cfDNA using the pre-amplification protocol.

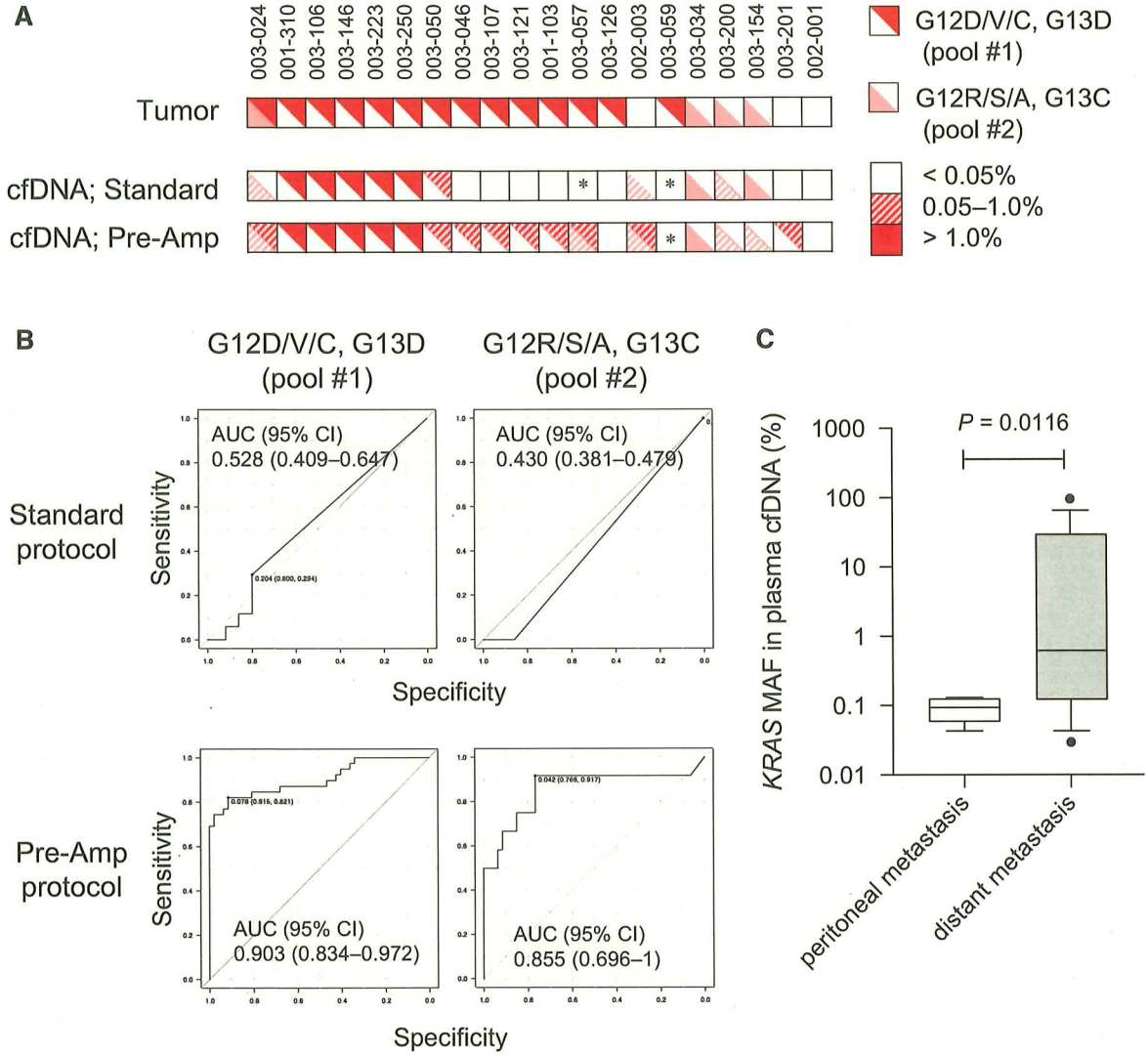

Fig. 2 Comparison between standard and modified dPCR protocols for detecting mutant *KRAS* in plasma cfDNA. **a** Results of the dPCR assay with and without pre-amplification (Pre-Amp) for 20 patients with unresectable PDA, in whom *KRAS* mutations were evaluated using fine-needle aspirates. Asterisk indicates samples with no result owing to the limited yield of plasma cfDNA for specific measurements. **b** ROC curve analysis of *KRAS* MAF accuracy for predicting the presence of mutation-containing resectable PDA (n = 17) relative to that in controls (n = 50) using the modified dPCR method. **c** Differences in *KRAS* MAF in plasma cfDNA between PDA cases with locally advanced or peritoneal metastasis (n = 7) and those with metastasis to distant organs (n = 18). Supplementary Tables 1 and 2 show the results of *KRAS* MAF for each sample

Mutation detection assays were then performed to test plasma cfDNA samples in the 112 IPMN follow-up cases. Owing to the lack of tumor DNA data in these cases, the results are shown as the positive call from either probe pool#1 or #2. Assembled data of the driver mutations in plasma cfDNA among the four populations, i.e., controls, IPMN, resected, and unresectable PDA, supported the trend hypothesis whereby the mutation call may increase step-wise for each category during tumor progression (Table 2). A significant fraction of the patients in the FN, WF, and HRS subsets exhibited > 0.1% positivity for mutant *KRAS* ($P < 0.0001$ vs. controls); however, *KRAS* MAF in plasma cfDNA from the WF and HRS groups was not higher than that of FN (Fig. 4b, Supplementary Table 4). Patient sample *GNAS* MAF values were also arranged with control values as a reference without a cut-off line, owing to the limited number of surgically resected *GNAS* mutant tumors. The values did not significantly differ among the IPMNs, regardless of the imaging-based tumor grade (Fig. 4c). A subset of patients with normal CA19-9 were characterized by high *KRAS* and *GNAS* MAF in plasma cfDNA, even in the absence of malignant features in imaging findings, and level increases were associated with the emergence of concomitant PDA or IPMN progression (Supplementary Figs. 8 and 9).

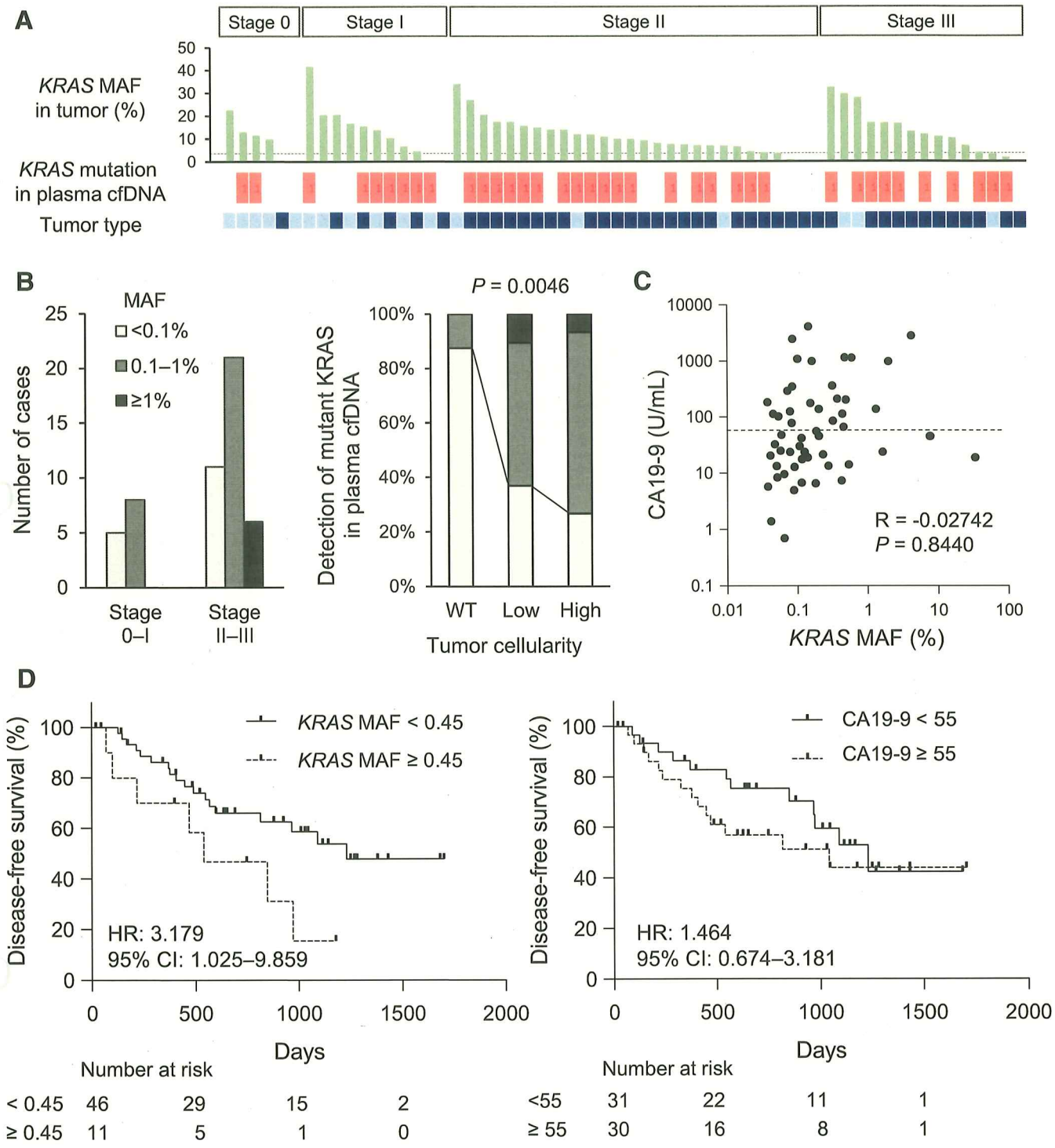

Fig. 3 Summary of *KRAS* mutation status in tumor tissue and plasma cfDNA. **a** *KRAS* mutation status in plasma cfDNA, and pathological stage (top row) and MAF in tumor specimens (green bars). Red boxes represent cases with positive *KRAS* mutation calls in plasma cfDNA by the modified dPCR protocol. Light and dark blue boxes indicate the tumor types; i.e., IPMN-associated PDA and PDA without IPMN, respectively. **b** *KRAS* gene mutation calls in plasma cfDNA for each stage. Number of positive cases along with *KRAS* MAF by the modified dPCR assay (left). *KRAS* mutation relationship between tumor tissue and plasma cfDNA. *KRAS* MAF in tumor tissue suggestive of tumor cellularity is categorized into three groups: wild-type (WT < 2.5%), low (2.5–10%), and high (> 10%) (right). **c** Correlation of *KRAS* MAF prior to surgical resection and CA19-9 levels. Dashed line indicates the cut-off level of 55 U/mL. **d** Kaplan–Meier analysis of plasma cfDNA *KRAS* MAF and CA19-9 level relation to disease-free survival

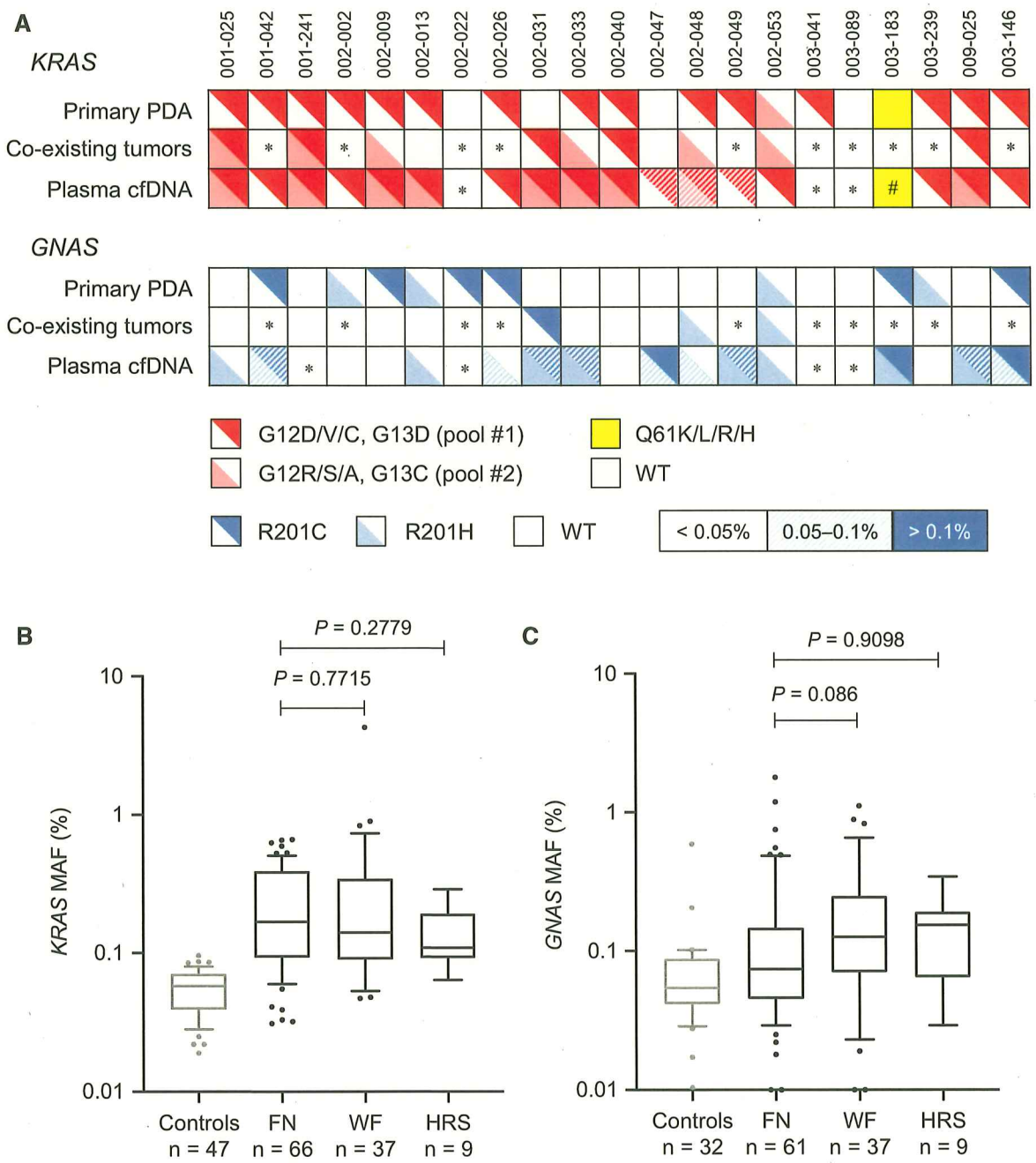

Fig. 4 Summary of plasma cfDNA mutation profiles in patients with IPMN. **a** Hot-spot mutation detection accuracy in *KRAS* and *GNAS* between tumor specimens and plasma cfDNA in IPMN-related pancreatic cancer. Boxes represent cases with positive *KRAS* or *GNAS* mutation calls. Mutation call levels are shown according to the MAF; 0.05–0.1% (striped) and over 0.1% (solid). Asterisks and pound signs indicate cases with no available data and dPCR assay results with pre-amplification of the codon 61 mutation, respectively. **b**, **c** Modified dPCR assay results for three categories: HRS, WF, and FN, with regard to malignant IPMN prediction. The numbers of cases listed represent those for which data were successfully obtained. Dotted lines indicate the positive *KRAS* mutation call cut-off as determined in Fig. 2b. Data were compared between groups using the Mann–Whitney *U* test

Discussion

Validation of the dPCR-based assay for patients with PDA and IPMN of various grades as categorized by imaging modalities [16, 17] supports its potential as a feasible, cost-effective, and sensitive tool for genetics-based diagnostics of pancreatic tumors with prognostic relevance and for surveillance. CfDNA can provide information regarding several aspects of cancer including genetics, tumor burden, and progression [4]; however, the low yield, even in patients with advanced stage disease, presents formidable challenges for its clinical utilization. Here we demonstrated the utility of plasma cfDNA measurement and genotyping of driver mutations in pancreatic neoplasms. Fluorescence-

Table 2 Results of mutation detection in tumor and plasma cfDNA of patients and participants

	Healthy volunteers $n = 76$	IPMN $n = 112$	Resectable PDA $n = 66$	Unresectable PDA $n = 30$	P value[b]
KRAS mutation in PDA					
G12D/G12V/G12R/other/WT/NA	–	–	23/13/20/2/8	8/5/3/1/3/10	–
GNAS mutation in PDA					
R201C/R201H/WT/NA	–	–	5/4/52/5	1/1/16/12	–
%MAF in plasma cfDNA (IQR)[a]					
KRAS pool#1	0.057 (0.0368–0.0685)	0.128 (0.0851–0.3442)	0.146 (0.0844–0.3861)	0.114 (0.0614–4.4101)	< 0.0001
KRAS pool#2	0.029 (0.0208–0.0440)	0.087 (0.0484–0.2101)	0.090 (0.0470–0.2733)	0.256 (0.1140–1.5842)	< 0.0001
GNAS R201C + R201H	0.054 (0.0410–0.0880)	0.091 (0.0453–0.1962)	0.1597 (0.0493–0.2772)	15.56 (7.8089–23.319)	0.0051

IQR interquartile range, *MAF* mutant allele frequency, *NA* data not available

[a]Data shown only for histologically proven resectable and unresectable PDAs, where tumor genotyping results were available

[b]Jonckheere–Terpstra test

combined with PCR-based cfDNA quantification may provide a tool to predict the likelihood of having tumors. Additionally, through use of an improved dPCR protocol that overcomes subsampling errors via a robust noise reduction effect termed pre-amplification [14], we confirmed more accurate detection of the hallmark mutations of pancreatic tumorigenesis in patients with resectable PDA along with a subset of individuals with IPMN potentially carrying an increased risk to develop invasive tumors.

We found that nuclear (e.g., *HBB*) and mitochondrial DNA (mtDNA; e.g., *MT-ND1*) copy numbers mutually associated with disease progression. Fluorescence assay-based cfDNA measurements closely correlated with nuclear DNA copy number but not mtDNA, indicating that circulating mtDNA levels may constitute an independent factor. Increased cfDNA levels were observed even in patients with IPMN, suggesting that the process of cfDNA release via apoptosis, necrosis, and secretion may not reflect a specific event in malignant tumors. Moreover, clinical IPMN grades did not reveal step-wise cfDNA increase, suggesting cfDNA as independent from imaging for predicting tumor burden and grade. Quantification of the nuclear and mitochondrial-derived cfDNA may, however, be beneficial toward predicting survival in patients with resectable pancreatic cancer, whereas this value appears to be lost for the later stages of the disease.

Low plasma cfDNA yield impedes early cancer diagnosis using standard techniques including via highly sensitive dPCR-based assays [10, 14]. However, a simple and low-cost "pre-amplification" modification significantly improved sensitivity (Fig. 2), allowing *KRAS* mutation detection accuracy in resectable PDA approaching that of conventional clinical tests [22, 23]. Compared to the CA19-9 score (< 55 U/mL in 33 of 86 PDA cases; 38.3%), plasma mutant *KRAS* status was captured in 22 patients (66.7%) by dPCR with pre-amplification. Given the limitations of early detection and the presence of a Lewis-negative genotype (lacking CA19-9) in approximately 6.9% of cases [24], the use of an alternative biomarker such as *KRAS* in plasma cfDNA is essential for accurately diagnosing PDAs.

The high Stage 0–I tumor cfDNA detection sensitivity may derive from relatively rich tumor cellularity in IPMN-associated cancer, indicative of low invasiveness. As PDA exhibits low tumor cellularity with cancer-associated fibroblasts (desmoplastic reactions), dPCR-based genotyping for driver genes using plasma cfDNA may not recognize small solid PDAs with abundant desmoplasia. Furthermore, the primary PDA and plasma cfDNA mutation profiles were occasionally discordant in patients with resected IPMN. Plasma-limited mutations partly derived from co-existing IPMN and pancreatic intraepithelial neoplasia in the normal-appearing pancreas. Therefore, plasma cfDNA genotyping can uncover rare variants not detected from the index tumor [25]. More detailed histological and genetic assessment of "background" lesions in the apparently normal pancreas, which are independent and distant from the clinically noticeable "index" invasive lesion, may provide better concordance of the mutation profile between plasma cfDNA and tumor DNA. The diagnostic accuracy of liquid biopsy using plasma in early-stage PDA remains

challenging [10, 26]; thus, alternative biospecimens containing higher amounts of tumor-derived nucleic acid obtained from lesion-adjacent regions, such as pancreatic and duodenal juice, may facilitate more precise tumor genotyping [27].

This study was limited owing to lack of follow-up for patients with IPMN. A significant fraction of these patients, even those with no Fukuoka factors (74.2%; 49/66), exhibited levels above the cut-off for *KRAS* MAF (> 0.1%) in plasma cfDNA as determined by the results from patients with pancreatic cancer and healthy volunteers. Prospective assessment of this subset may support the refinement of the current guideline for IPMN that assigns high priority to the morphological evaluation of imaging findings. Because IPMN comprises multicentric/synchronous lesions rather than a single locoregional disease, quantitatively and qualitatively evaluating *KRAS* and *GNAS* mutations and tumor suppressor genes may allow better whole pancreas surveillance in these patients [4]. The more frequent capture of mutant *KRAS* than *GNAS* in plasma cfDNA (Fig. 4b, c) despite the absence of a definitive *GNAS* MAF cut-off is supported by our previous demonstration that IPMN precursors more frequently show mutant *KRAS* in the normal-appearing pancreas [19]. Moreover, in the current study, the variant types captured by the *KRAS* and *GNAS* probe pools were not specified owing to the limited plasma cfDNA yield. However, given the significant recent improvement of reagents for dPCR allowing multiplex analysis, it is technically possible to determine the variants of multiple genes in a single target enrichment using dPCR (e.g., *KRAS* plus *TP53* and *SMAD4*) [28]. Such an approach will take full advantage of the benefits of pre-amplification. Finally, we primarily utilized a classic cfDNA blood collection method; our findings should thus be confirmed using high-quality biomaterial without a freeze–thaw step [29].

Defining risk stratification methodology for early pancreatic cancer detection is of considerable clinical concern [2]. Here, we demonstrated that a combination of different cfDNA measurements provides a detailed profile in patients with pancreatic neoplasms. The modified dPCR assay to reduce subsampling error can detect driver mutations at earlier stages and may complement imaging and standard tumor markers. Such screening of tumor suppressors involved in pancreatic tumorigenesis may enhance protocol accuracy; moreover, our data may promote reform of the current algorithm for IPMN surveillance, which mainly depends upon imaging studies, and provide an additional cost-effective clinical test to assess tumor burden and metastatic potential.

Acknowledgements We thank Munehiko Ogata and Mayumi Suzuki (Sapporo Higashi Tokushukai Hospital) for genetic analysis technical support; Akio Matsushita (Shibetsu City Hospital), Takuya Sugimura (Teine-Keijinkai Hospital), and Eiko Aoyanagi (Sapporo Higashi Tokushukai Hospital) for clinical sample collection and tissue sample preparation; other members of the Department of Gastroenterology at Asahikawa Medical University and Institute of Biomedical Research laboratory staff at Sapporo Higashi Tokushukai Hospital for helpful suggestions throughout the course of this project and critical reading of the manuscript. Y. M. and Y. Ono receive funding from Hitachi High-Tech Corporation. The other authors declare no potential conflicts of interest.

References

1. Kanda M, Matthaei H, Wu J, et al. Presence of somatic mutations in most early-stage pancreatic intraepithelial neoplasia. Gastroenterology. 2012;142:730–9.
2. Patra KC, Bardeesy N, Mizukami Y. Diversity of precursor lesions for pancreatic cancer: the genetics and biology of intraductal papillary mucinous neoplasm. Clin Transl Gastroenterol. 2017;8:e86.
3. Gormally E, Vineis P, Matullo G, et al. TP53 and KRAS2 mutations in plasma DNA of healthy subjects and subsequent cancer occurrence: a prospective study. Cancer Res. 2006;66:6871–6.
4. Suenaga M, Yu J, Shindo K, et al. Pancreatic juice mutation concentrations can help predict the grade of dysplasia in patients undergoing pancreatic surveillance. Clin Cancer Res. 2018;24:2963–74.
5. Wu J, Matthaei H, Maitra A, et al. Recurrent GNAS mutations define an unexpected pathway for pancreatic cyst development. Sci Transl Med. 2011;3:92ra66.
6. Furukawa T, Kuboki Y, Tanji E, et al. Whole-exome sequencing uncovers frequent GNAS mutations in intraductal papillary mucinous neoplasms of the pancreas. Sci Rep. 2011;1:161.
7. Berger AW, Schwerdel D, Costa IG, et al. Detection of hot-spot mutations in circulating cell-free DNA from patients with intraductal papillary mucinous neoplasms of the pancreas. Gastroenterology. 2016;151:267–70.
8. Wan JCM, Massie C, Garcia-Corbacho J, et al. Liquid biopsies come of age: towards implementation of circulating tumour DNA. Nat Rev Cancer. 2017;17:223–38.
9. Bettegowda C, Sausen M, Leary RJ, et al. Detection of circulating tumor DNA in early- and late-stage human malignancies. Sci Transl Med. 2014;6:224ra24.
10. Takai E, Totoki Y, Nakamura H, et al. Clinical utility of circulating tumor DNA for molecular assessment in pancreatic cancer. Sci Rep. 2015;5:18425.
11. Hadano N, Murakami Y, Uemura K, et al. Prognostic value of circulating tumour DNA in patients undergoing curative resection for pancreatic cancer. Br J Cancer. 2016;115:59–655.
12. Cohen JD, Li L, Wang Y, et al. Detection and localization of surgically resectable cancers with a multi-analyte blood test. Science. 2018;359:926–30.
13. Kinde I, Wu J, Papadopoulos N, et al. Detection and quantification of rare mutations with massively parallel sequencing. Proc Natl Acad Sci USA. 2011;108:9530–5.
14. Ono Y, Sugitani A, Karasaki H, et al. An improved digital polymerase chain reaction protocol to capture low-copy KRAS mutations in plasma cell-free DNA by resolving 'subsampling' issues. Mol Oncol. 2017;11:1448–58.
15. Rowlands V, Rutkowski AJ, Meuser E, et al. Optimisation of robust singleplex and multiplex droplet digital PCR assays for

high confidence mutation detection in circulating tumour DNA. Sci Rep. 2019;9:12620.
16. Tanaka M, Fernandez-Del Castillo C, Kamisawa T, et al. Revisions of international consensus Fukuoka guidelines for the management of IPMN of the pancreas. Pancreatology. 2017;17:738–53.
17. Del Chiaro M, Verbeke C, Salvia R, et al. European experts consensus statement on cystic tumours of the pancreas. Dig Liver Dis. 2013;45:703–11.
18. Brierley JD, Gospodarowicz MK, Wittekind C. TNM classification of malignant tumours. 8th ed. Hoboken: Wiley-Blackwell; 2017.
19. Omori Y, Ono Y, Tanino M, et al. Pathways of progression from intraductal papillary mucinous neoplasm to pancreatic ductal adenocarcinoma based on molecular features. Gastroenterology. 2019;156:647–81.
20. Gemenetzis G, Bagante F, Griffin JF, et al. Neutrophil-to-lymphocyte ratio is a predictive marker for invasive malignancy in intraductal papillary mucinous neoplasms of the pancreas. Ann Surg. 2017;266:339–45.
21 Kim J, Bamlet WR, Oberg AL, et al. Detection of early pancreatic ductal adenocarcinoma with thrombospondin-2 and CA19–9 blood markers. Sci Transl Med. 2017;9:eaah5583.
2. Liu R, Chen X, Du Y, et al. Serum microRNA expression profile as a biomarker in the diagnosis and prognosis of pancreatic cancer. Clin Chem. 2012;58:610–8.
23. Madhavan B, Yue S, Galli U, et al. Combined evaluation of a panel of protein and miRNA serum-exosome biomarkers for pancreatic cancer diagnosis increases sensitivity and specificity. Int J Cancer. 2015;136:2616–27.
24. Luo G, Liu C, Guo M, et al. Potential biomarkers in Lewis negative patients with pancreatic cancer. Ann Surg. 2017;265:800–5.
25. Koldby KM, Mortensen MB, Detlefsen S, Pfeiffer P, Thomassen M, Kruse TA. Tumor-specific genetic aberrations in cell-free DNA of gastroesophageal cancer patients. J Gastroenterol. 2019;54:108–21.
26. Sikora K, Bedin C, Vicentini C, et al. Evaluation of cell-free DNA as a biomarker for pancreatic malignancies. Int J Biol Mark. 2015;30:e136–e141141.
27. Okada T, Iwano H, Ono Y, et al. Utility of "liquid biopsy" using pancreatic juice for early detection of pancreatic cancer. Endosc Int Open. 2018;6:E1454–E14611461.
28. Jackson JB, Choi DS, Luketich JD, et al. Multiplex preamplification of serum DNA to facilitate reliable detection of extremely rare cancer mutations in circulating DNA by digital PCR. J Mol Diagn. 2016;18:235–43.
29. Schmidt B, Reinicke D, Reindl I, et al. Liquid biopsy—performance of the PAXgene(R) blood ccfDNA tubes for the isolation and characterization of cell-free plasma DNA from tumor patients. Clin Chim Acta. 2017;469:94–8.

Data Supplement for

Digital PCR-based Plasma Cell-free DNA Mutation Analysis for Early-Stage Pancreatic Tumor Diagnosis and Surveillance

Okada T, et al.

This PDF file includes:

Supplementary Methods

Supplementary Figures 1–10

Supplementary Methods

Sample Collection, Storage, and Processing

Patients and healthy volunteers were enrolled in seven participating institutions: Sapporo Higashi Tokushukai Hospital, Shonan Kamakura General Hospital, Teine-Keijinkai Hospital, Shibetsu City Hospital, Chiba Tokushukai Hospital, Hokkaido University Hospital, and Asahikawa Medical University Hospital. All participants were Japanese. Healthy volunteers were defined as individuals who showed no evidence of tumors during annual medical checkups (e.g., chest X-ray and abdominal ultrasound for all volunteers and gastrointestinal endoscopy for individuals older than 40 years of age).

We collected blood samples (limited to 16 mL) at the time of diagnosis and prior to any surgical procedures and neoadjuvant chemotherapy using 8-mL tubes containing EDTA-2K (SPM-L1008EMS; Sekisui Medical, Co., Ltd., Tokyo, Japan), and gentle inversion. CA19-9 values and neutrophil-to-lymphocyte ratio measurements were evaluated per routine examination. In particular, blood was obtained from patients with severe jaundice and cholangitis following biliary stenting. The cell-free plasma was prepared using two centrifugation steps within 1 h after blood drawing: 1,100 × *g* for 10 min at 20–25°C, then 18,000 × *g* for 10 min at 4°C, and stored at −80°C until shipped using dry ice. Cell-Free DNA BCT (Streck, La Vista, NE) was also utilized after September 2016, with which the blood samples could be shipped at room temperature within seven days after collection without the requirement of rapid processing and losing a portion of the cfDNA (Supplementary Figure 10). All samples were processed at the Molecular Genetics Laboratory in Sapporo Higashi Tokushukai Hospital. CfDNA was

isolated from the plasma using a QIAamp Circulating Nucleic Acids Kit (Qiagen, Valencia, CA), eluted in 100 μL volume, and immediately quantified using a Qubit dsDNA HS Assay Kit with a Qubit2.0 fluorometer (Thermo Fisher Scientific, Boston, MA). Different cfDNA concentration between the EDTA tube and Streck BCT was adjusted according to the regression equation based on the measurements (Supplementary Figure 10). CfDNA quantification was also performed by measuring the copy number of nuclear (i.e., hemoglobin β-subunit gene; *HBB*) and mitochondrial DNA (mitochondrially encoded NADH:ubiquinone oxidoreductase core subunit 1 gene; *MT-ND1*) using digital polymerase chain reaction (dPCR). All assay primers and probes are listed in Supplementary Table 5.

Representative formalin-fixed paraffin-embedded (FFPE) blocks of the surgically resected primary tumor were selected for each case to include the viable invasive compartment with high tumor cell content, and genomic DNA was then purified from the corresponding unstained slides using a GeneRead DNA FFPE Kit (Qiagen, Hilden, Germany). For unresected PDAs, FFPE specimens obtained by endoscopic ultrasound-guided fine needle biopsy were employed. For some genomic DNA samples isolated from the FFPE sections, targeted amplicon sequencing using the Ion AmpliSeq Custom Next-Generation Sequencing DNA Panels was also employed as described previously.[1]

Mutation Detection by dPCR

Mutant *KRAS* variants (codons 12/13 and 61) and *GNAS* variants (codon 201) were analyzed using a QX200 Droplet Digital PCR System (Bio-Rad, Hercules, CA) either

using standard or modified protocols as previously described.[2] Briefly, custom locked nucleic acid-based probes and primers were designed for eight hot-spot mutations in *KRAS* codons 12 (G12D, G12V, G12R, G12C, G12A, and G12S) and 13 (G13D and G13C) (Integrated DNA Technology (IDT), Inc., Coralville, IA). Two sets of probes for four *KRAS* variants (pool #1 for G12D, G12V, G12C, and G13D; pool #2 for G12A, G12R, G12S, and G13C) labeled with 6-fluorescein amidite (FAM) in combination with the probe for the wild-type *KRAS* labeled with hexachloro-fluorescein (HEX) were utilized for the assay as previously described (Supplementary Table 6A).[1] A ddPCR KRAS Q61 Screening Kit (Bio-Rad) was utilized for *KRAS* codon 61 mutations. To capture the GNAS R201C/H mutations, an additional primer/probe set was constructed. The sequences are presented in Supplementary Table 6A. The reaction mixture was prepared as described in Supplementary Table 6B. Purified genomic DNA was partitioned into approximately 22,000 droplets per sample by mixing with 70 µL Droplet Generation Oil in a QX200 droplet generator (Bio-Rad). Droplets were then subjected to thermal cycling, as described in Supplementary Table 6C. Samples were transferred to a QX200 droplet reader (Bio-Rad) for fluorescence measurement. Droplets were scored as positive or negative based on their fluorescence intensity, which was determined by the gating threshold defined using nuclease free water as the negative control. We confirmed the positive detection using gBlocks Gene Fragments (approximately 180 bp; IDT). Finally, absolute copy number input in the reaction and the ratio of the mutated fragment were calculated using QuantaSoft (ver 1.7; Bio-Rad) software based on the Poisson distribution. Plasma cfDNA samples were scored as positive for mutation when at least three mutant droplets/reaction were detected by ddPCR, and mutant allele

frequency was calculated. The primary tumor DNA isolated from the viable area in FFPE blocks was determined as mutation positive when the allele frequency was > 2.5%. For IPMN-related PDA, additional non-invasive compartments such as co-existing IPMN and PanINs in the normal appearing pancreas from resected specimens were also analyzed.

In the modified assay termed "pre-amplification," the reactions were prepared in a total volume of 22 μL containing 9.3 μL of purified cfDNA (equivalent to cfDNA from 186 μL plasma) to amplify the *KRAS* Exon 2 and *GNAS* Exon 8 target allele using the primer set same as dPCR detection. Eight pre-amplification cycles followed by a second-run dPCR were sufficient to obtain approximately 5,000–10,000 amplified copies/ng cfDNA, allowing an increase in the sensitivity of mutation detection and the signal-to-noise ratio.[2] We performed multiple rounds of pre-amplification (typically 3–4 times) to avoid missing detectable mutations in the low-yield of the patient's plasma cfDNA. The reaction mixtures were then diluted with TE buffer (pH 8.0), vigorously mixed with equal volumes of chloroform (FUJIFILM Wako Pure Chemical Corporation, Osaka, Japan) by vortexing and pipetting, and centrifuged; the aqueous phase was separated, and the amplified DNA was then purified using a DNA Clean & Concentrator-5 kit (Zymo Research Corporation, Orange, CA). DNA was finally eluted using 12 μL of elution buffer, and we utilized 4 μL of the refined products for subsequent second-run dPCR to detect mutations (duplicates or triplicates). For the *KRAS* mutation in codon 61, pre-amplification was performed using a primer set unique to Exon 3, and the detection was employed by the ddPCR™ KRAS Q61 Screening Kit (Bio-Rad) (see

Supplementary Figure 7 for further details). The average of positive mutation calls was calculated based on the analysis.

Supplementary Data References

1. Omori Y, Ono Y, Tanino M, et al. Pathways of progression from intraductal papillary mucinous neoplasm to pancreatic ductal adenocarcinoma based on molecular features. Gastroenterology. 2019;156:647-61 e2.
2. Ono Y, Sugitani A, Karasaki H, et al. An improved digital polymerase chain reaction protocol to capture low-copy KRAS mutations in plasma cell-free DNA by resolving 'subsampling' issues. Mol Oncol. 2017;11:1448-58.

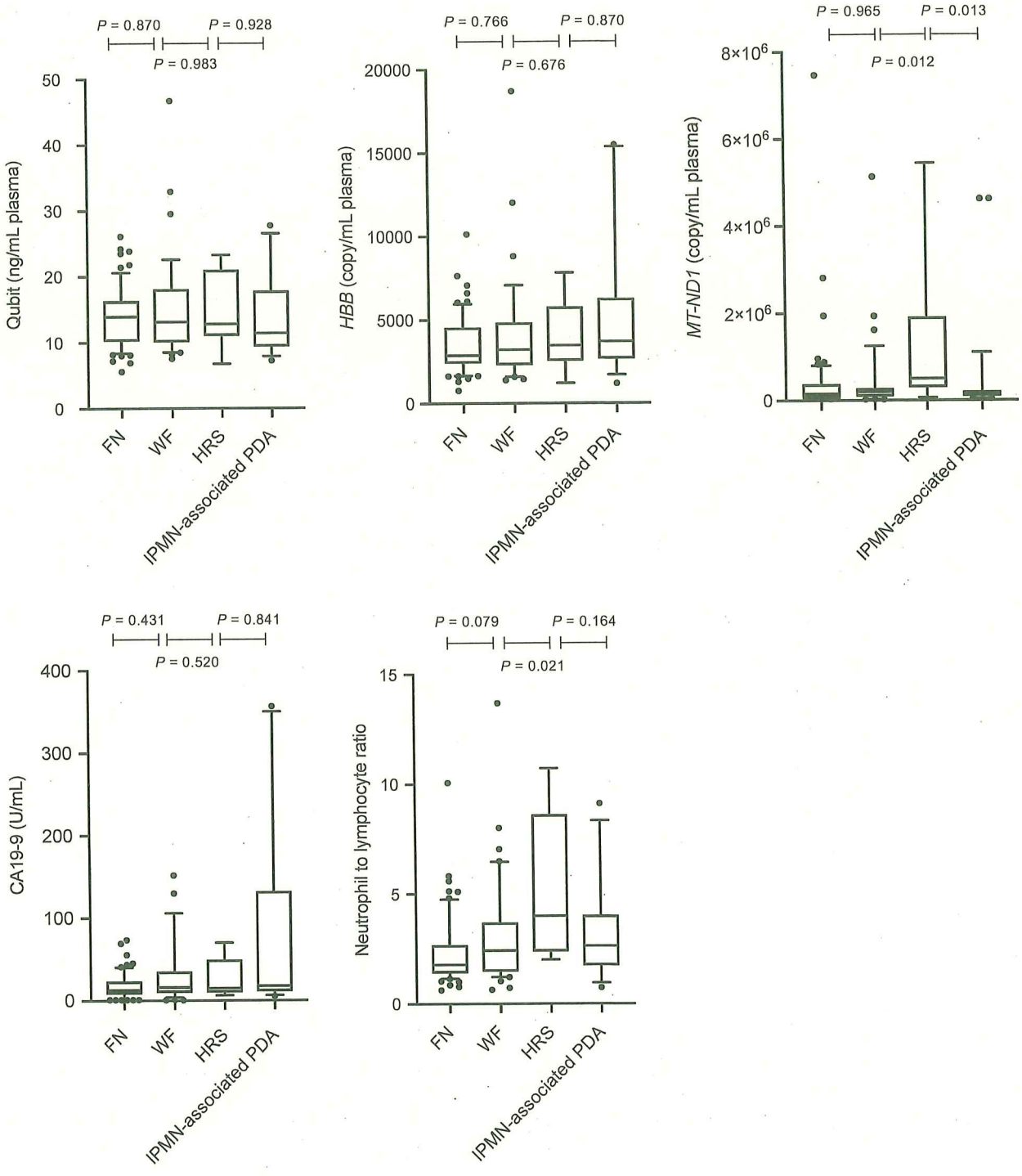

Supplementary Figure 1
Results from plasma cfDNA, CA19-9, and neutrophil to lymphocyte ratio measurement analysis for four categories; i.e., FN with no risk factor, HRS, WF, and IPMN-associated PDA. The box-and-whiskers graphs show median, interquartile, and 10–90% ranges.

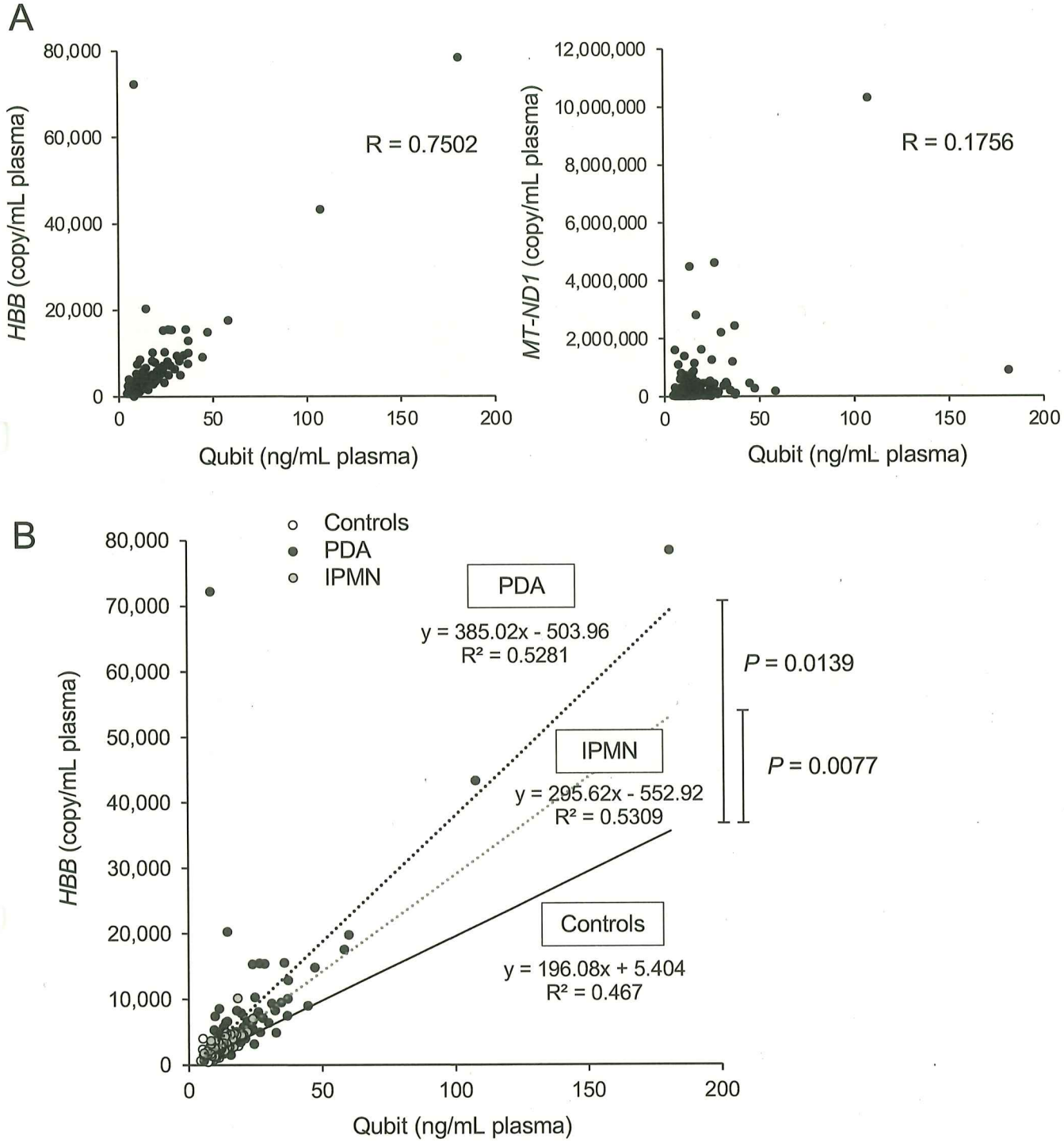

Supplementary Figure 2

A, Correlation between Qubit measurement and dPCR-based quantification assay (*HBB*, *MT-ND1*) results. B, Correlation between Qubit and HBB in three categories: Control, IPMN, and PDA. Dots represent PDA (filled circles), PDA (gray circles), and healthy individuals (open circles). Linear regression analysis was performed to detect correlations; the regression equations and predicted R^2 values are shown.

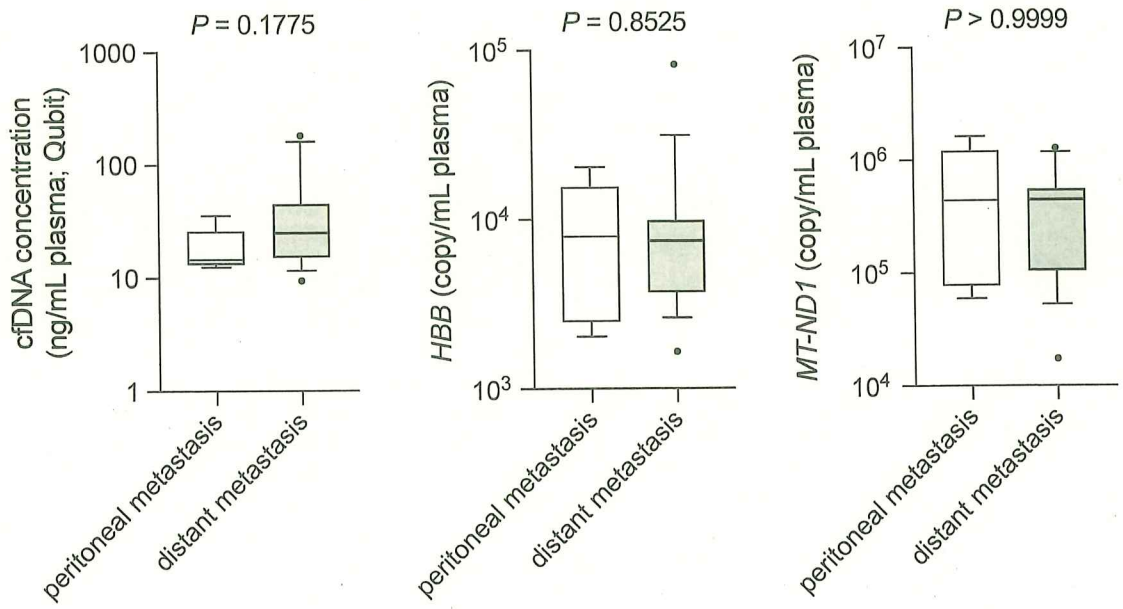

Supplementary Figure 3

Comparison of plasma cfDNA measurements between patients with PDA exhibiting peritoneal (n = 7) and distant metastasis (n = 17). The box-and-whiskers graphs show median, interquartile, and 10–90% ranges.

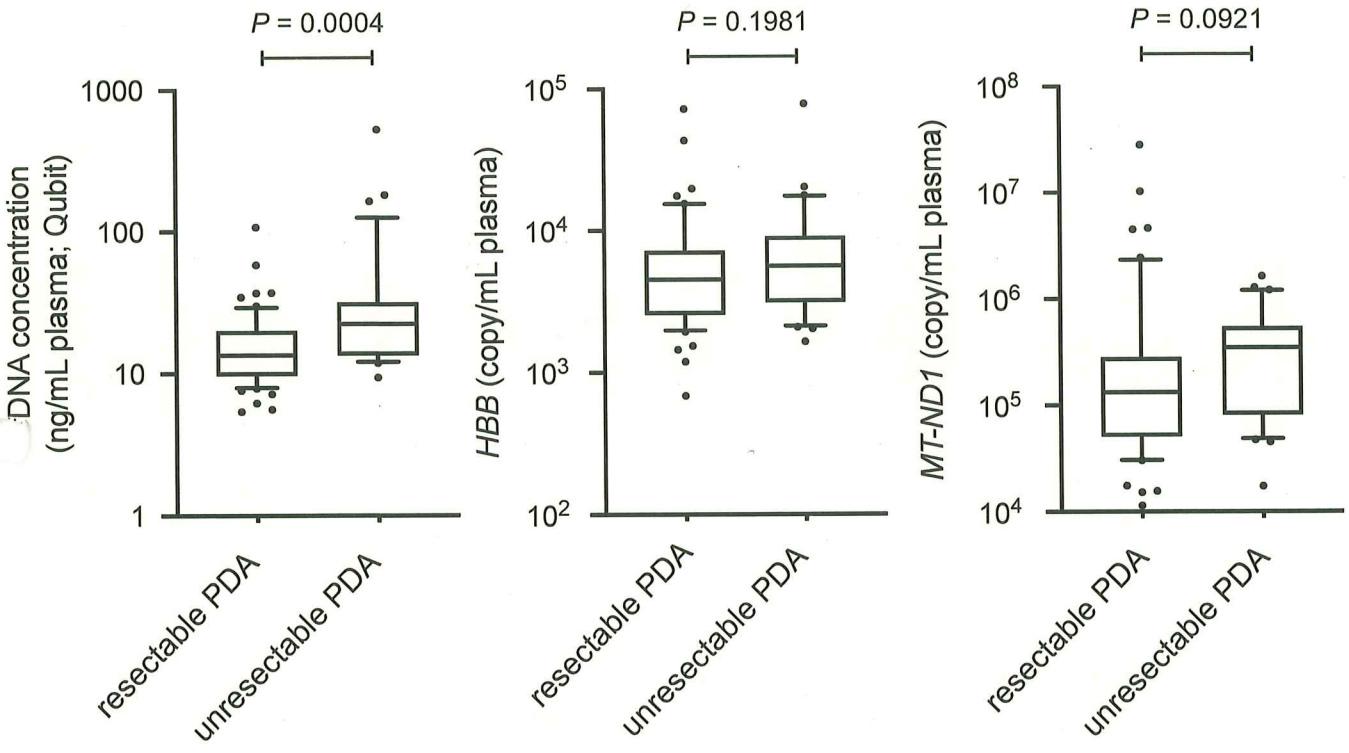

Supplementary Figure 4
Comparison of cfDNA measurements between resectable and unresectable PDA.

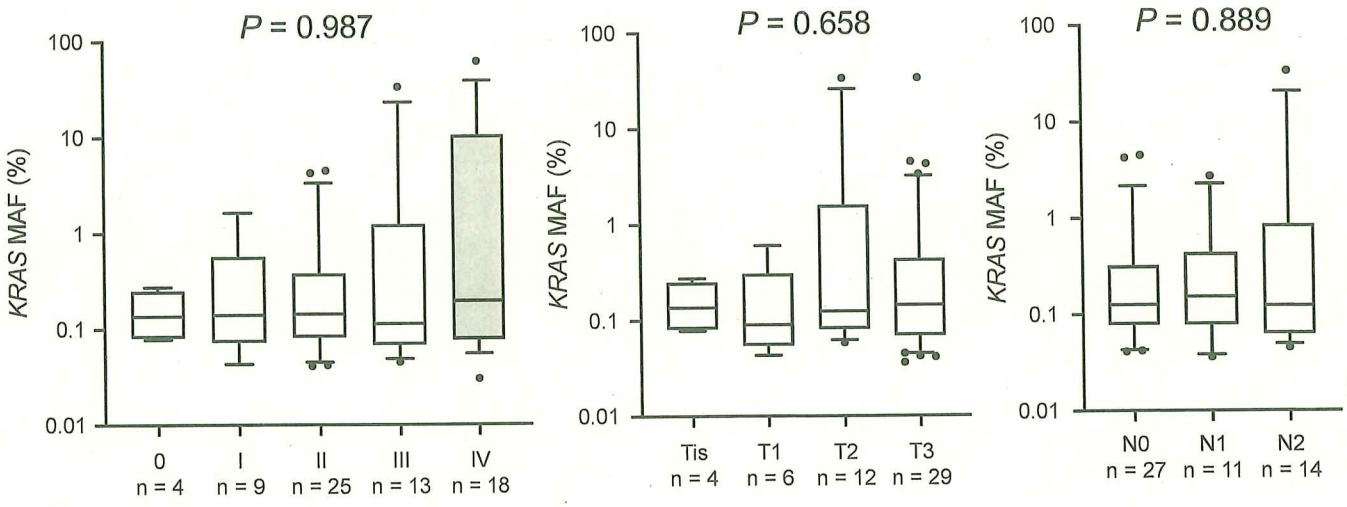

Supplementary Figure 5

KRAS MAF is shown based on classification of the stage of PDAs carrying *KRAS* mutations at codon 12/13 or 62 (*left*). The values for each pT- (*middle*) and pN-factor (*right*) are indicated for the cases with resectable PDAs harboring mutant *KRAS* (Stage 0–III). Significance was determined by Jonckheere-Terpstra test

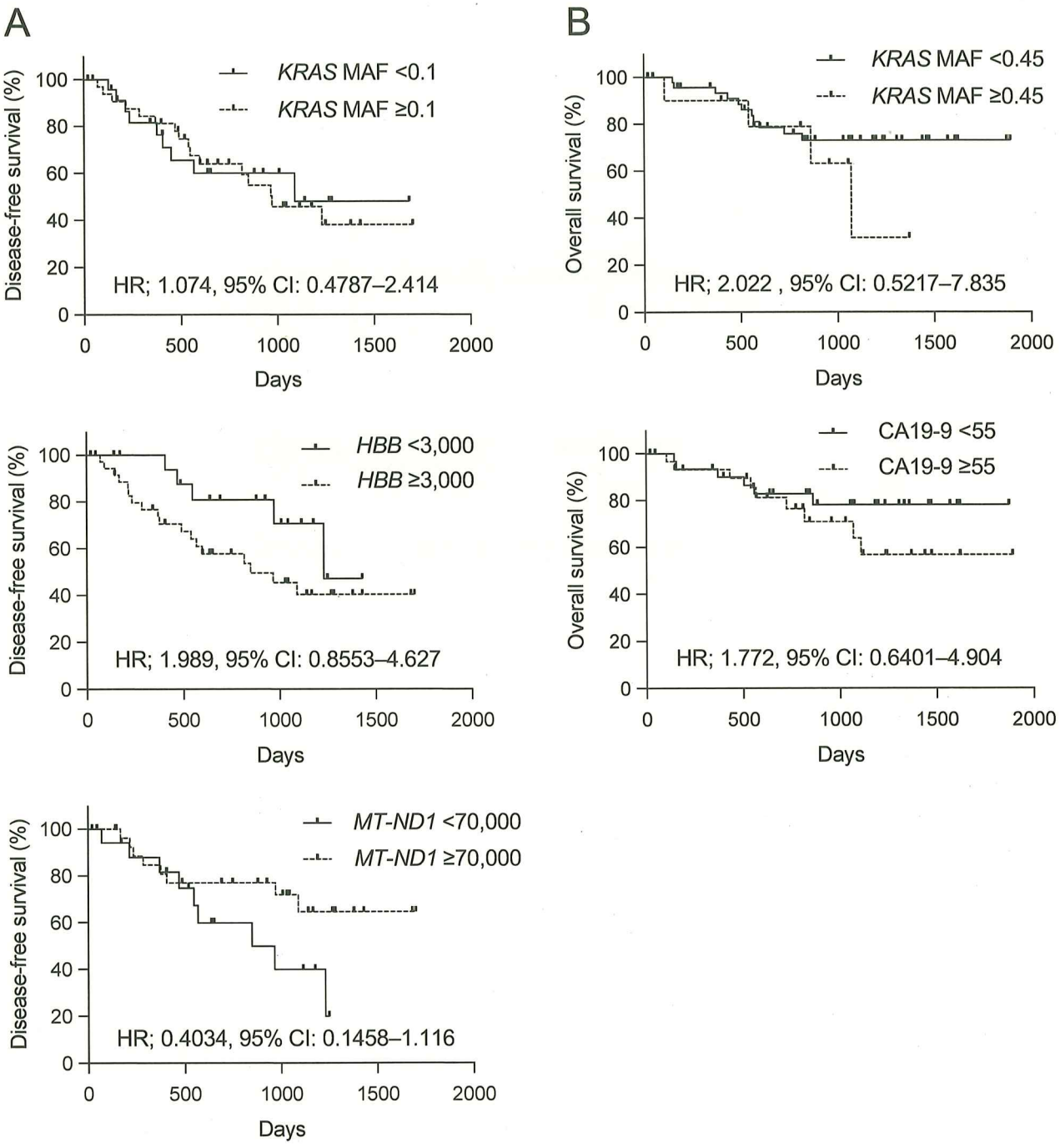

Supplementary Figure 6

A. Kaplan–Meier analysis of the relationship of *KRAS* MAF (top panel), *HBB*- (middle panel), and *MT-ND-1* copy numbers (bottom panel) with disease-free survival. The cut-off values were determined based on the results shown in Fig 2 (*KRAS* MAF) and Fig 1B, C (*HBB* and *MT-ND1*, respectively).

B. Kaplan–Meier analysis of the relationship of *KRAS* MAF (top panel) and CA19-9 levels (bottom panel) with overall survival.

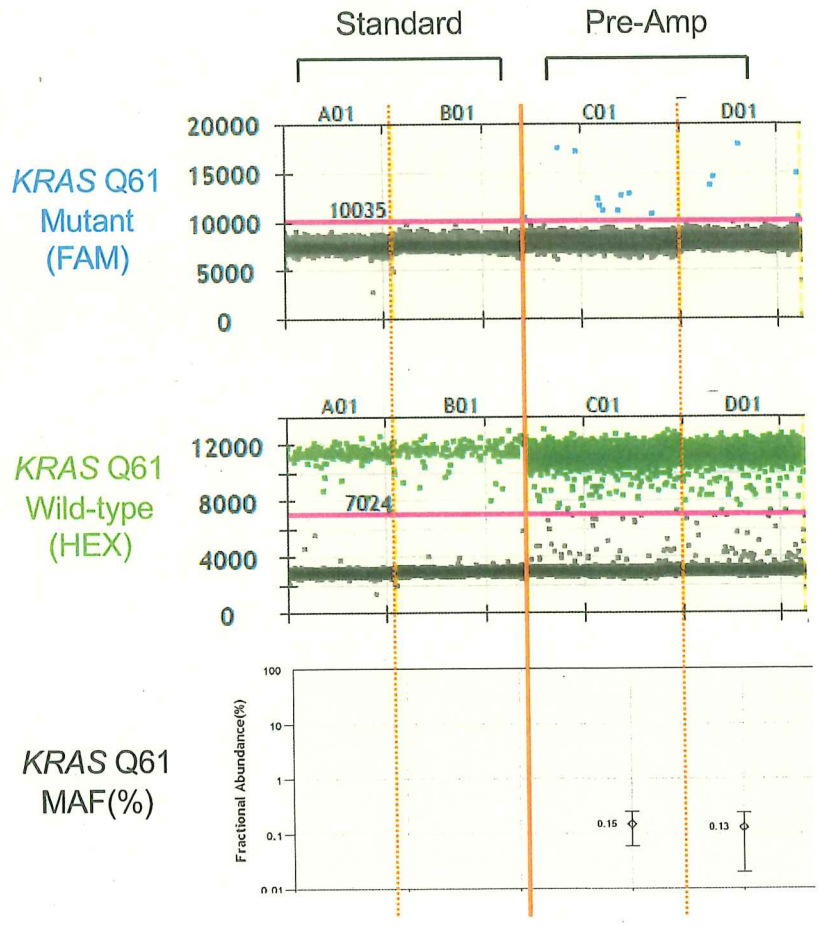

Supplementary Figure 7

Plasma cfDNA from case 18 with IPMN-associated PDA harboring the *KRAS* Q61 mutation (Table S2) was subjected dPCR assay with and without pre-amplification. The assay was performed in duplicate by ddPCR using the ddPCR™ *KRAS* Q61 Screening Kit (Bio-Rad). Upper and middle panels indicate fluorescence intensities for wild-type (HEX; green dots) and mutant *KRAS* (FAM; blue dots); the MAF is shown in the lower panel.

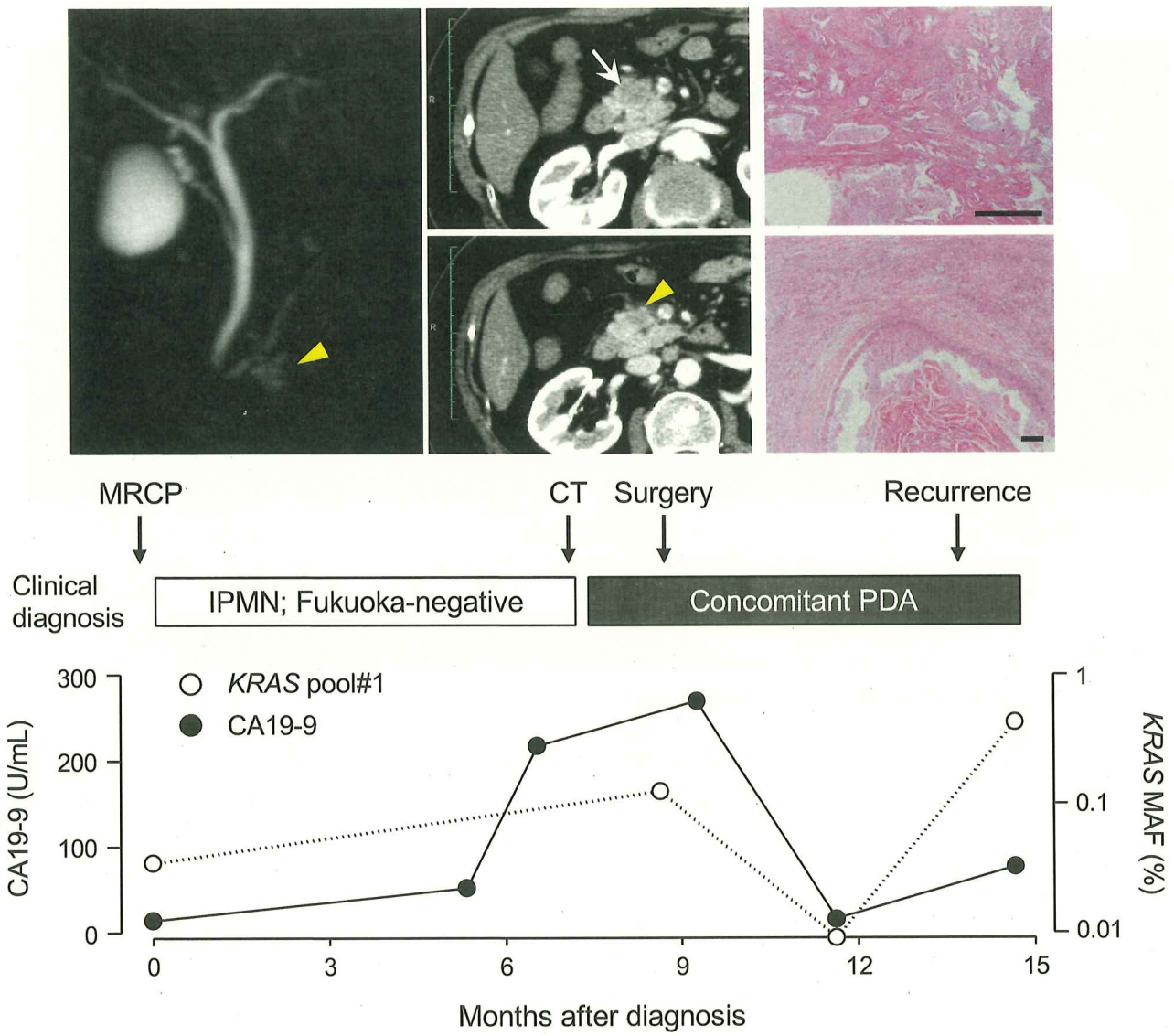

Supplementary Figure 8

Magnetic resonance cholangiopancreatography (MRCP) demonstrated a small cystic lesion (arrowhead, upper left) in the head of the pancreas at the time of diagnosis (patient #005-045). Six months later, computed tomography (CT) showed a solid tumor beside the cyst (arrow, upper middle), which was classified as a well-differentiated adenocarcinoma (upper, right; scale bars, 500 μm). Time course of CA19-9 level and *KRAS* mutation allele frequency (MAF) in plasma cfDNA are shown in the lower panel.

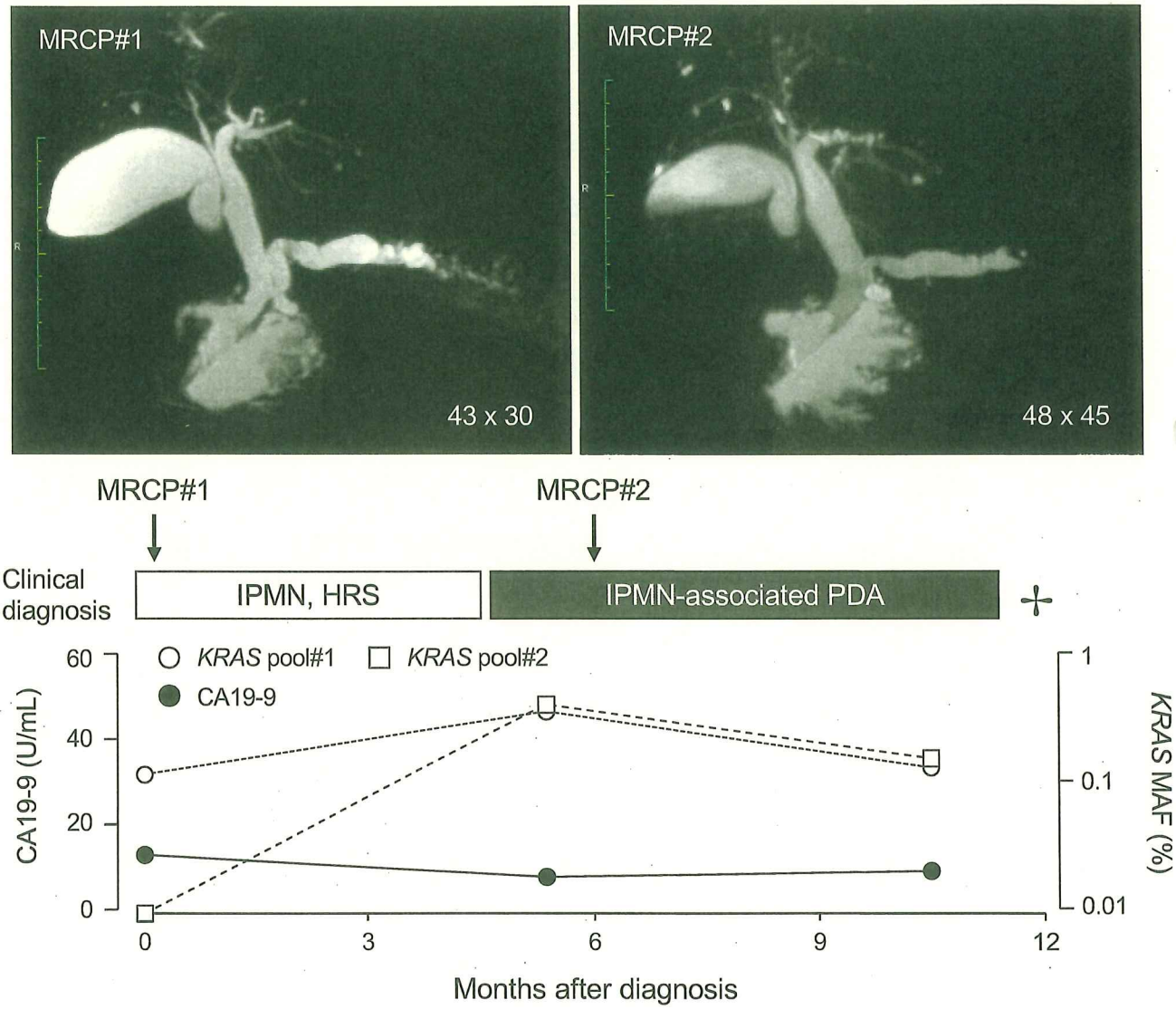

Supplementary Figure 9

Magnetic resonance cholangiopancreatography (MRCP) demonstrated a large cystic lesion with mural nodules and significant dilatation of the main pancreatic duct in the head of the pancreas, suggestive of high-risk stigmata, at the time of diagnosis (patient #005-036; upper left). Six months later, enlargement of the cyst with outline irregularity was observed, suggesting duodenal leakage (upper right). Time course of CA19-9 level and *KRAS* mutation allele frequency (MAF) in plasma cfDNA are shown in the lower panel. The patients missed the chance for surgical resection of the tumor owing to sudden death from a cause unrelated to IPMN.

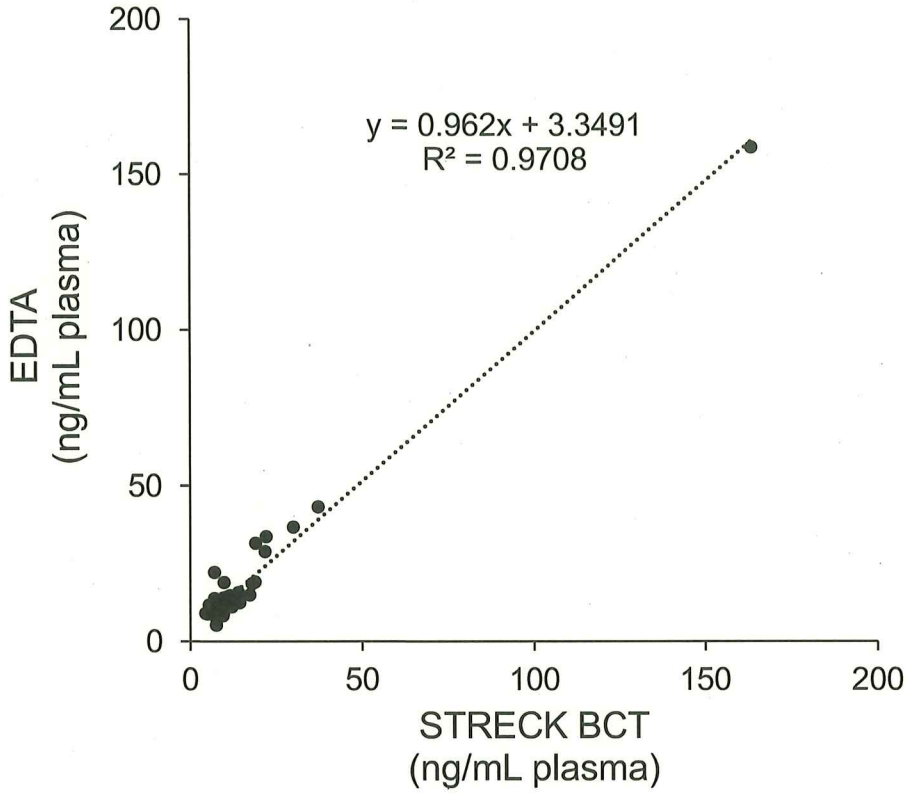

Supplementary Figure 10
Relationship between cfDNA concentration from plasma collected with tubes containing EDTA-2K and STRECK BCT. Linear regression based on 50 samples from both healthy volunteers and patients is shown.

補足データ（Supplementary Table）は、
下記リンクよりダウンロード下さい
http://link.springer.com/article/10.1007/s00535-020-01724-5